JOURNAL OF MATERIALS SCIENCE 23 (1988) 2607–2612

Correlation of dynamic friction and the dislocation etch pit density surrounding annealed scratches in (1 1 1) p-type silicon

DAE-SOON LIM,* STEVEN DANYLUK
Department of Civil Engineering, Mechanics and Metallurgy, University of Illinois at Chicago, Chicago, Illinois 60680, USA

The dynamic friction coefficient between a 90° pyramid diamond and a (1 1 1) p-type silicon single crystal has been measured for linear, unidirectional scratches made in the [1 1 0] direction in laboratory air, deionized water and ethanol. The friction coefficient for grooves formed in air increased from 0.6 to 0.7 as the number of scratches increased, reaching a steady state value after ten scratches. The friction coefficient for grooves formed in deionized water and ethanol decreased from 0.7 to 0.5 and also reached a steady state value after ten scratches. Scanning electron microscopy showed that the groove morphology depended on the fluid in contact with the surface during the scratch test. The grooves formed after ten scratches were annealed to 750° C for 3600 sec and etch pits were measured as a function of distance from the groove wall. The etch pit density and their distance from the groove wall was related to the type of fluid used in the scratch test: the density was highest and the distance from the groove wall largest for the groove formed in air and lowest for the groove formed in ethanol. These results imply that the deformation mode and the magnitude of the residual stresses surrounding the groove depend on the enviromental conditions during the scratch test. The friction coefficient was found to vary linearly with the average etch pit density.

1. Introduction

Single-crystal silicon undergoes a considerable amount of mechanical deformation during the fabrication of electronic circuits [1, 2]. Single-crystal boules are cut into thin, flat wafers by diamond-impregnated cut-off wheels which are flooded by lubricating fluids. Fluids flush away the debris and, lubricate and cool the contact region between the silicon and abrasive wheel surfaces. This mechanical processing generates cracks, microtwins and dislocations on the silicon surfaces and the depth of this damage limits the thickness of the wafers [3, 4]. Wafering causes the most severe damage, usually representing approximately 10% of the wafer thickness [5]. This damage must be removed because it degrades the electrical properties and may be the source of catastrophic brittle failure in the subsequent processing. Lapping and polishing, processes in which fixed- or loose-abrasive particles, suspended in a fluid, are used to remove wafering damage. Lapping and polishing damage is less severe than wafering and any remaining damage is sometimes removed by chemical etching which is the final step prior to device fabrication. When the device fabrication is completed, each is removed by scribbing or dicing the perimeter of the device with a diamond impregnated tool or wheel. The scribbing and dicing re-introduces damage at the perimeter of the finished electronic device.

Mechanical damage and deformation is the result of stresses that are transmitted by the abrasive to the silicon surface [6]. As the abrasive scratches the silicon surface, compressive and tensile stresses result at the leading and trailing edges of the abrasive [7–9]. The compressive stresses generate dislocations and the tensile stresses produce microcracks which propagate on cleavage planes at large distances beyond the immediate contact zone. The loads on the abrasive particle and the fluid are two variables that determine the mode and extent of the damage generated in the silicon surface and as a result, these variables predetermine the wear rate and the amount of damage. In addition, the mechanical damage and deformation also results in residual stresses that surround the wear track of a particular abrasive. These residual stresses contribute to wear because tensile residual stresses would aid in crack propagation and compressive residual stresses aid the generation and propagation of dislocations. The annealing of wear tracks relieves these residual stresses because the damage is redistributed with the addition of thermal energy. It is this interrelationship between the damage and the residual stresses that is critical in the strength and fracture toughness of single-crystal silicon.

This paper is an extension of our previous work in which single-crystal silicon wafers were abraded by a Vicker's pyramid diamond [10]. Here we describe the

Present address: National Bureau of Standards, Ceramics Division, Tribology Group, Gaithersburg, Maryland 20899, USA.

0022–2461/88 $03.00 + .12

measurement of the dynamic friction coefficient of (1 1 1) p-type single-crystal wafers and the correlation of the mean value of the friction coefficient with the dislocation density of dislocation etch pits that surround an annealed scratch. The friction coefficient is a parameter which is closely related to damage and wear through the deformation mode and the residual stresses in the damage region. We show the correlation of the dynamic friction coefficient to the dislocation etch pit density and the influence of three environments on this damage. Deionized water is used as a benchmark to which the results of air and ethanol are compared.

2. Experimental details

Linear slow speed scratches were made a 90° pyramidal diamond on oriented single-crystal wafers. The specimens were 102 mm diameter, 0.5 mm thick, p-type (1 1 1) single-crystal wafers supplied by the Monsanto Electronic Materials Company. Each wafer was lapped and polished according to semiconductor industry standards and scribbed and fractured into 77.2 × 19.3 mm rectangular plates. These plates were dipped in a 10 vol % hydrofluoric acid bath for 30 sec, rinsed in deionized water and dried. The samples were then immersed in either deionized water or ethanol for the scratch test. One set of samples was scratched in laboratory air with a relative humidity of 50% with a fluid contacting the surface. The silicon geometry was chosen such that the long axis was [1 1 0].

The samples are mounted on a platen and secured by spring tabs. An instrumented 90° pyramidal diamond is attached to a fixture that is mounted with linear bearings. A motor assembly drives the dead-weighted diamond and two strain gauges record the deflection of the diamond as it forms a linear scratch [9]. The dead weight on the diamond was chosen for convenience as 0.49 N in all the results reported in this paper. This load was found in previous work to be below a threshold at which plastic deformation occurs [10]. The strain gauge output is recorded directly into a microcomputer which converts this output into a tangential force. The velocity of the diamond was 2.28×10^{-2} m sec^{-1} so as to minimize frictional heating during the test and the length of the traverse was typically 50 mm. Fig. 1 shows a schematic diagram of the silicon and diamond and a scanning electron micrograph of an edge-on view of the diamond situated on a silicon surface. The diamond tip had a nominal radius of 10×10^{-6} m and there was no noticeable wear of the diamond as determined by SEM after the scratching tests.

The apparatus can be programmed for single or multiple uni- or multidirectional scratches and the dynamic friction coefficient can be measured throughout the duration of the test. The results reported here are for unidirectional scratches. The scratches were annealed at 750° C for 3600 sec and the silicon surfaces etched in a Modified CP4 solution to reveal dislocation etch pits. Each etch pit represents the termination of a dislocation and these were counted as a function of distance from the groove edge.

3. Results

Fig. 2 shows a typical scanning electron micrograph of the top view of a typical single scratch that was made in air. The micrograph shows conchoidal fracture that results from lateral cracks that propagate away from the contact zone and intersect the surface. The groove shows evidence of plastic deformation as well as cracks and the surrounding region contains debris particles that have been expelled from the groove. The

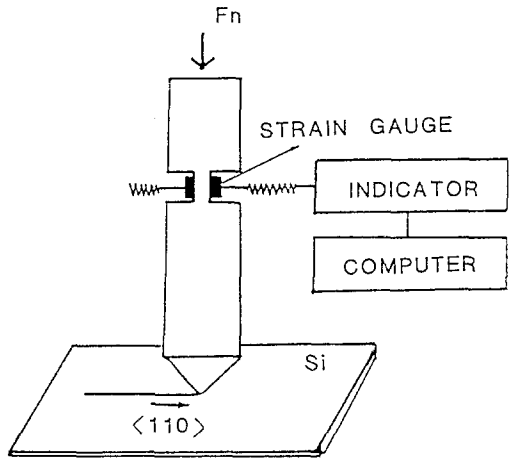

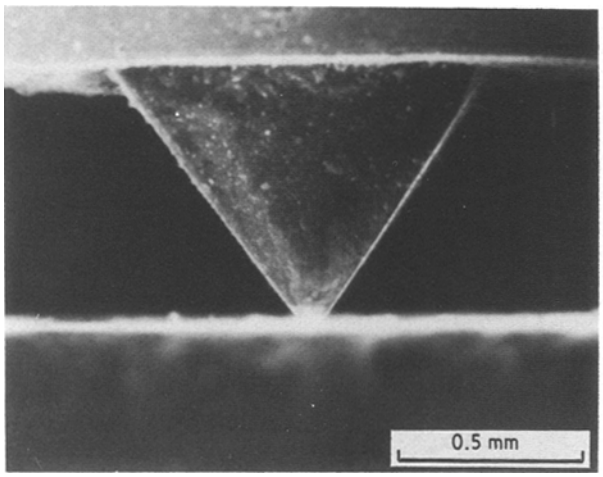

Figure 1 Schematic diagram of the automated dynamic friction apparatus and a scanning electron micrograph of a cross section of a diamond positioned on a silicon surface.

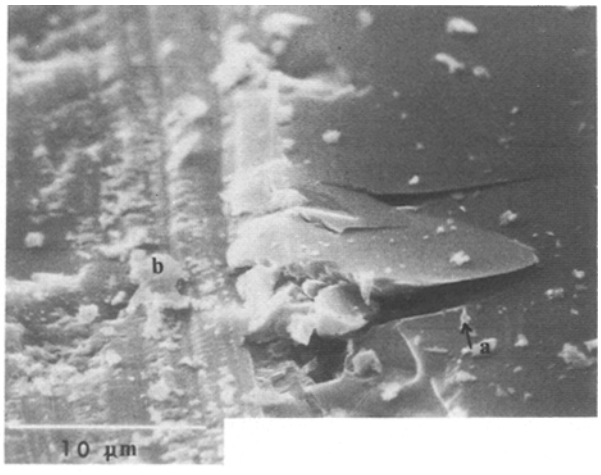

Figure 2 Scanning electron micrograph of a linear scratch formed in air by a 90° pyramidal diamond. (a) Typical deformed regions and (b) propagation of lateral cracks are shown.

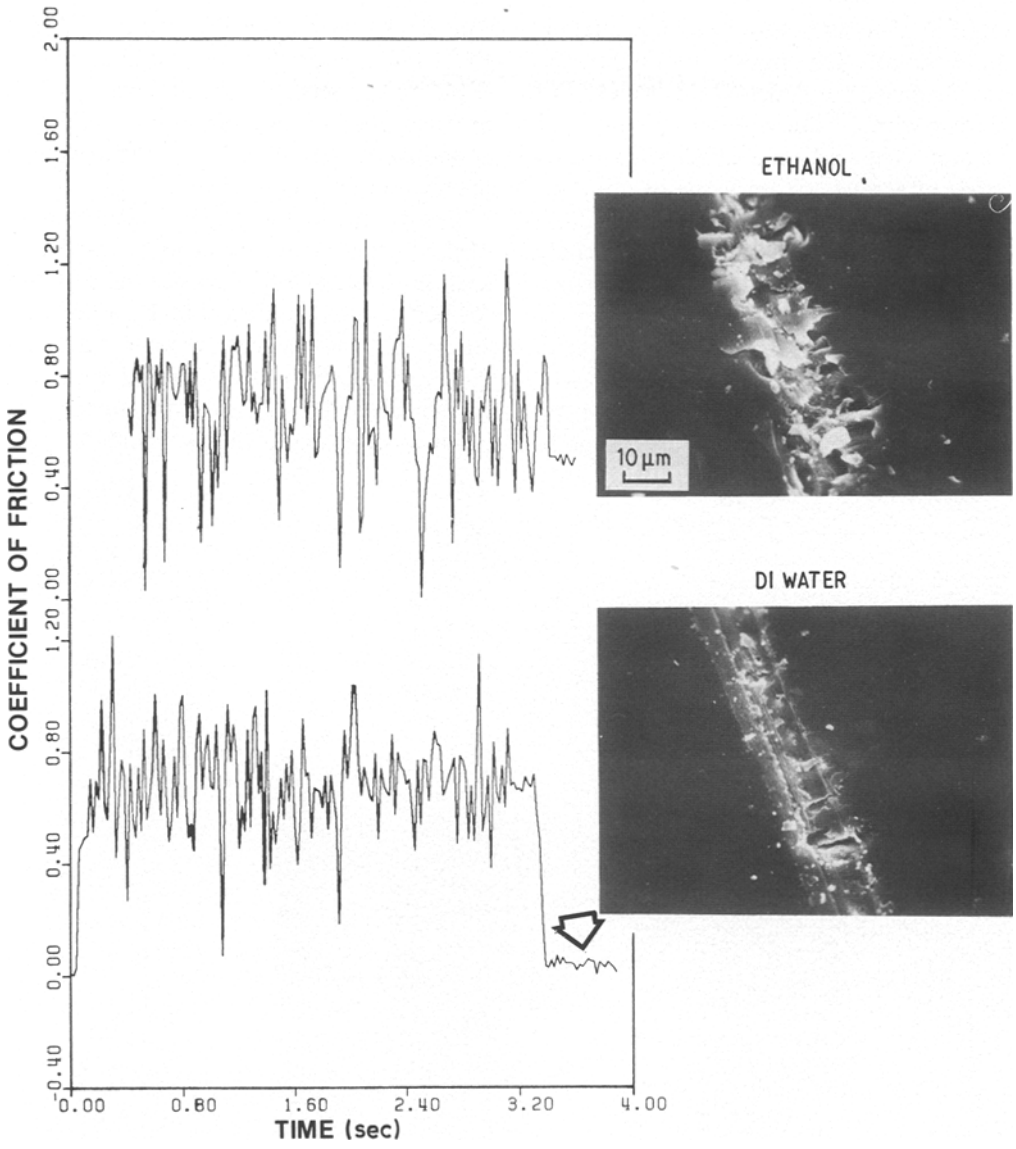

Figure 3 The dynamic friction coefficient traces as a function of scratching time of scratches formed in ethanol and deionized (DI) water. These data show the fluctuation about the mean and the noise (see the arrow in the figure) associated with the measurement equipment. The inset shows scanning electron micrographs of the groove surface.

cross-sectional area of the scratch can be measured and the wear rate can be determined as had been done in a previous study [7]. That work showed that ethanol enhances wear compared with deionized water. Fig. 3 shows two examples of the measured friction coefficient as a function of scratching time and the corresponding scanning electron micrographs of the scratched surfaces for single scratches formed in ethanol and deionized water. The scratching time corresponds to the time of travel of the diamond to form a single 30 mm long scratch. The friction coefficient traces show a considerable amount of scatter with a mean at approximately 0.7. This deviation about the mean is indicative of the deformation of the silicon because the uncertainty due to equipment noise is considerably smaller as shown in Fig. 3. The scanning electron micrographs show that the scratch morphology depends on the fluid as has been previously reported [7]. The scratch made in ethanol contains significantly more cracking and the groove width is generally larger than the scratch made in deionized water.

Fig. 4 shows the mean friction coefficient plotted

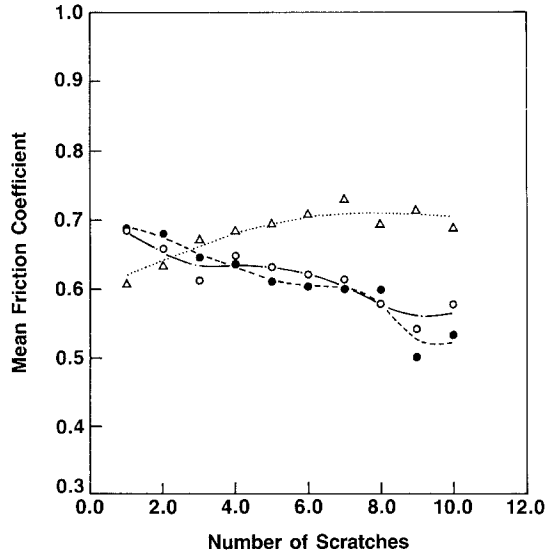

Figure 4 The mean friction coefficient plotted against the number of scratches. These data show that the friction coefficient reaches a steady state value after approximately ten scratches. (△) Air, (○) deionized water, (●) ethanol.

against the number of scratches formed in air, deionized water and ethanol. This figure shows that the mean friction coefficient for deionized water and ethanol are similar with a value of approximately 0.7 for the first scratch. The friction coefficient decreases with the number of scratches to a value of approximately 0.5 for the tenth scratch. The friction coefficient for air has a friction coefficient of approximately 0.6 for the first scratch and this value increases to a value of approximately 0.7 after ten scratches.

The linear scratches formed in each fluid were annealed and etched and Fig. 5 shows optical micrographs of the dislocation etch pits surrounding the groove formed after the tenth unidirectional scratch. This figure shows that the etch pits are aligned along the [1 1 0] at an angle of 60° as expected for a diamond cubic crystal structure. A number of reverse pile ups are also observed because the stress distribution surrounding the scratch provides the driving force for the dislocation propagation.

The dislocation density was measured as a function of the distance from the groove edge for the length of each groove and Fig. 6 shows the results for grooves formed by ten unidirectional scratches. This figure shows that the dislocation density is larger by about 20% and the dislocations extend approximately 20% further beyond the groove edge for the groove formed in air as opposed to the two fluids.

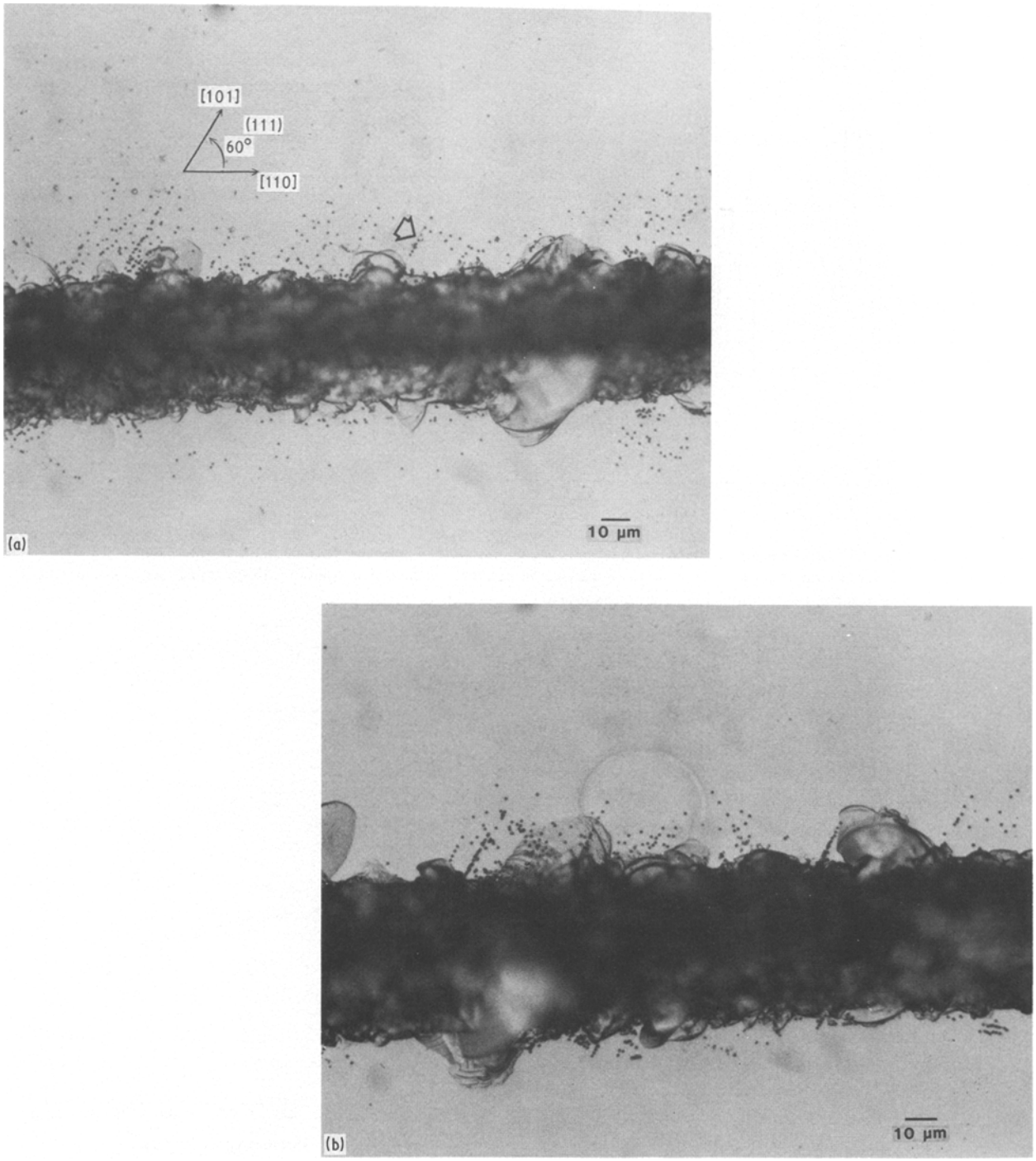

Figure 5 Optical micrographs of the annealed and etched grooves formed after ten scratches in (a) air, (b) deionized water, and (c) ethanol. Dislocations emanate from about the groove and propagate along the [1 1 0] slip directions. The dislocation density varies according to the fluid in contact with the surface during the scratch test. The arrow points to the reverse pile up of dislocation etch pits.

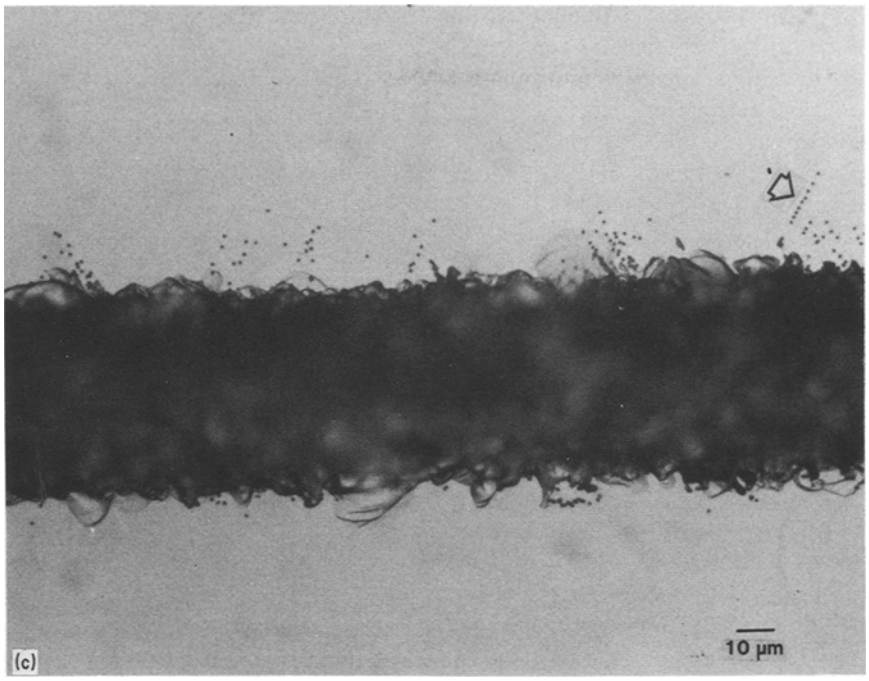

Figure 5 Continued.

4. Discussion

The results of the previous section have shown that the dynamic friction coefficient has considerable scatter about a mean value. These results indicate the changes in the deformation mode of the silicon and a more detailed description will be provided in a subsequent publication [11]. For the present discussion, we concentrate on the correlation of the mean value with the deformation mode and the dislocation etch pit density. The scanning electron micrographs shown in Fig. 3 indicate that the deformation mode is substantially different for the scratches made in ethanol and deionized water. The evidence of cracking for the scratches formed in ethanol indicates that the imposed stresses were relieved by microcracking so that dislocation generation and propagation would be suppressed in contradistinction to the scratch formed in deionized water. This result is reflected in Fig. 6 because the dislocation density is the lowest for the grooves formed in ethanol.

Two aspects of Fig. 6 should be emphasized. The dislocation density is highest for the groove formed in air and lowest for the groove formed in ethanol. This result is consistent with the observation that there is more cracking associated with the groove formed in ethanol compared to the grooves formed in the other two environments. In addition to the differences in the dislocation density, the distance from the groove edge is also consistently higher for the groove formed in air as compared to the groove formed in ethanol. This result is expected if the residual stresses are higher for the groove formed in air as compared to the grooves formed in the other two environments. Both results

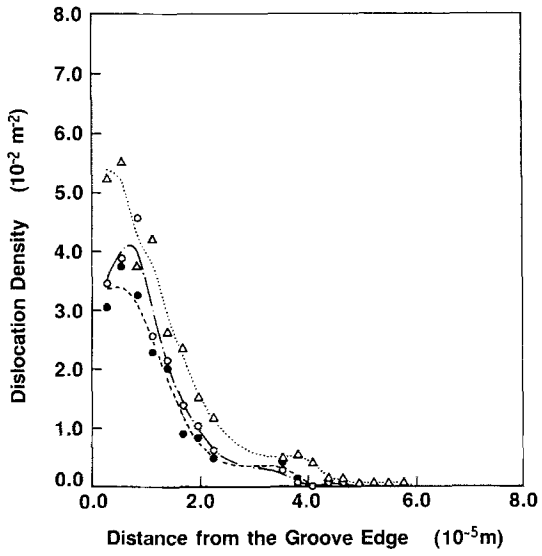

Figure 6 The dislocation density plotted against the distance from the groove edge for the annealed tenth groove. The magnitude of the density and the distance from the groove edge is largest for the groove formed in air and smallest for the groove formed in ethanol. (△) Air, (○) deionized water, (●) ethanol.

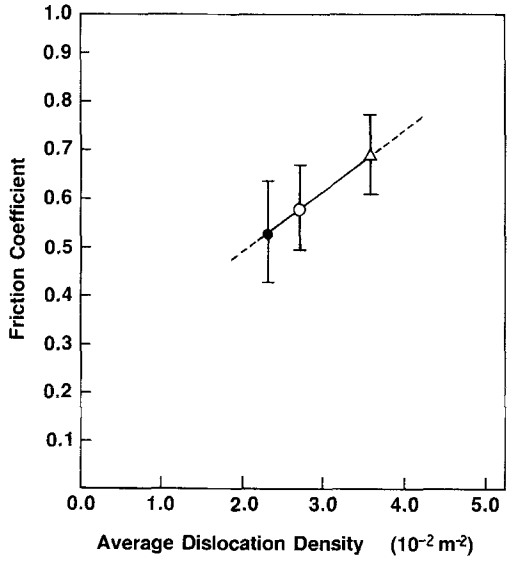

Figure 7 The friction coefficient plotted against the average dislocation density for grooves formed in (△) air, (○) deionized water and (●) ethanol.

imply a correlation between the dynamic friction coefficient and the dislocation density and Fig. 7 shows this correlation for the three environments. This figure shows the mean friction coefficient and the statistical deviation about the mean during the formation of the tenth scratch plotted against the average dislocation density obtained after annealing a groove formed of ten scratches. It is seen that there is a linear correlation between these two parameters with the highest friction coefficient and average dislocation density corresponding to the groove formed in air and the lowest to the groove formed in ethanol.

5. Conclusions

The results of this study show that a measurement of the dynamic friction coefficient reflects the deformation mode of single crystal silicon abraded by a 90° pyramidal diamond. The deformation mode and the dynamic friction coefficient are modified by environmental fluids as compared to scratches formed in air. The friction coefficient reaches an apparent steady state value after ten scratches: the friction coefficient increases from 0.6 to 0.7 for scratches formed in air and decreases from 0.7 to 0.5 for scratches formed in deionized water and ethanol. The mean dislocation density and the position of the dislocations relative to the groove edge varies with the environment during the scratch test. This implies that the density of dislocations and/or the residual stresses are modified by the presence of the fluids. As a result, there is a linear correlation between the dynamic friction coefficient and the average dislocation density.

Acknowledgements

This work was supported by the US Department of Energy under contract to the Jet Propulsion Laboratory, Flat-plate Solar Array Project no. 956053. This support is gratefully acknowledged. Special thanks are extended to K. M. Koliwad, M. Leipold, A. Morrison and C. P. Chen of JPL for support and encouragement through this study. Additional help was provided by J. Gramsas and C. Scott.

References

1. R. B. SOPER, "Silicon Device Processing", NBS Special Publication 337 (National Bureau of Standards, Washington, 1970) pp. 412, 419.
2. R. C. MEEK and M. C. HUFTSTUTLER Jr, *J. Electrochem. Soc.* **116** (1969) 893.
3. C. P. CHEN and M. H. LEIPOLD, Proceedings of the 15th IEEE Photovoltaic Specialists Conference, (1981) p. 1122.
4. T. S. KUAN, K. K. SHIH, J. A. VAN VECHTEN and W. A. WESTDROP, *J. Electrochem. Soc.* **127** (1980) 1387.
5. C. P. CHEN, *ibid.* **129** (1982) 2835.
6. A. G. EVANS, "The Science of Ceramic Machining and Surface Finishing II", NBS Special Publication 562 (US Department of Commerce Washington, D.C., 1979).
7. S. DANYLUK and J. L. CLARK, *Wear* **103** (1985) 149.
8. R. STICKLER and G. R. BOOKER, *Phil. Mag.* **8** (1963) 859.
9. D. S. LIM and S. DANYLUK, *J. Mater. Sci.* **20** (1985) 4084.
10. S. W. LEE, PhD thesis, University of Illinois at Chicago (1986).
11. D. S. LIM and S. DANYLUK, to be published.

Received 3 September
and accepted 1 December 1987